Electronic Supplementary Information

Using Post-synthetic Ligand Modification to Imprint Chirality onto the Electronic States of Cesium Lead Bromide ($CsPbBr_3$) Perovskite Nanoparticles

Gouranga H. Debnath,[1] Zheni N. Georgieva,[1] Brian P. Bloom,[1] Susheng Tan[2,3] and David H. Waldeck[1,3,*]

[1]Department of Chemistry, University of Pittsburgh, Pittsburgh, Pennsylvania 15260, United States

[2]Department of Electrical and Computer Engineering, University of Pittsburgh, Pittsburgh, Pennsylvania 15261, United States

[3]Petersen Institute of NanoScience and Engineering, University of Pittsburgh, Pittsburgh, Pennsylvania 15261, United States

E-mail: dave@pitt.edu

* To whom correspondence should be addressed.

Table of Contents

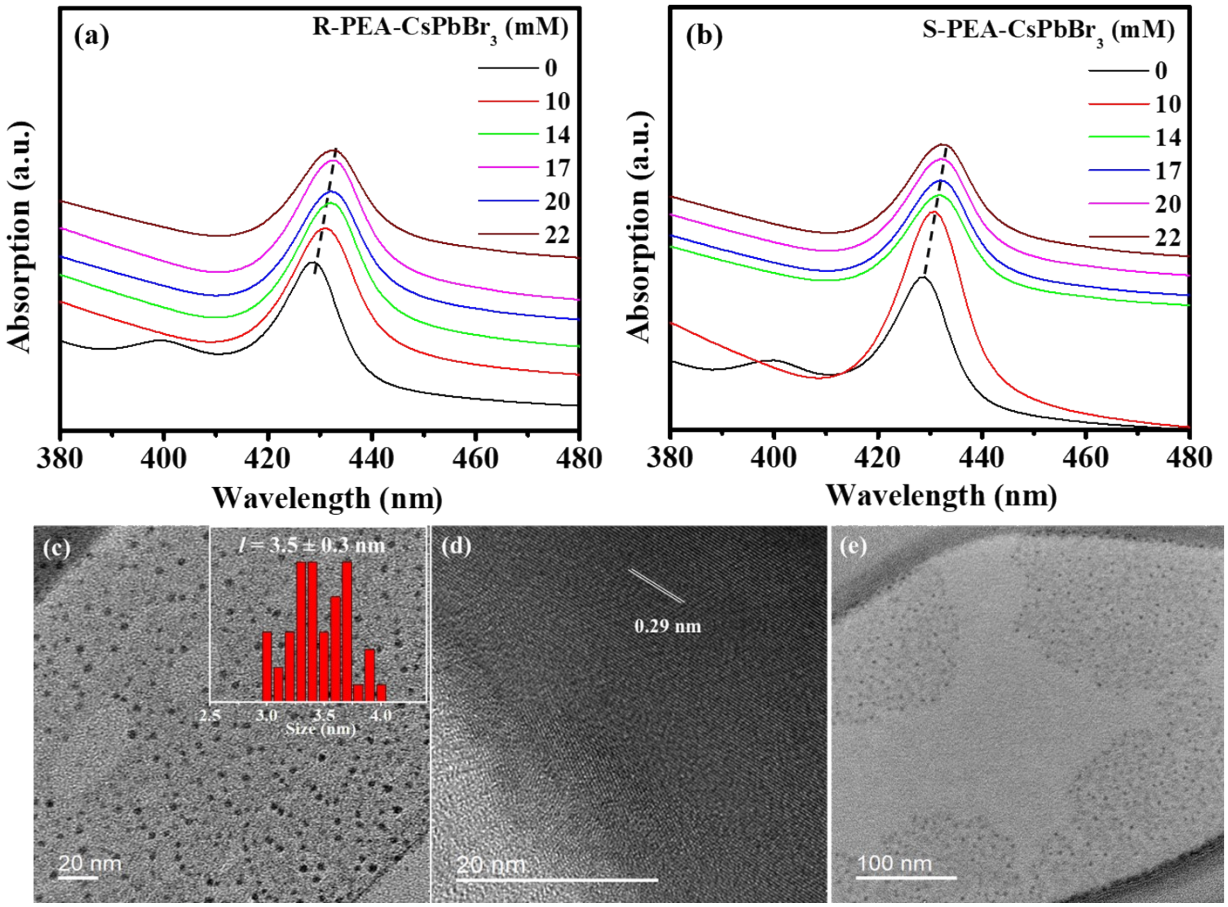

Figure S1. (a,b) UV-Vis absorption spectra of R- and S-PEA-$CsPbBr_3$ NPs with increasing PEA concentration is shown. The NPs were dispersed in toluene and are offset for clarity. (c-e) TEM images of R- PEA-$CsPbBr_3$ NPs with [PEA] = 20 mM in the NP dispersion.

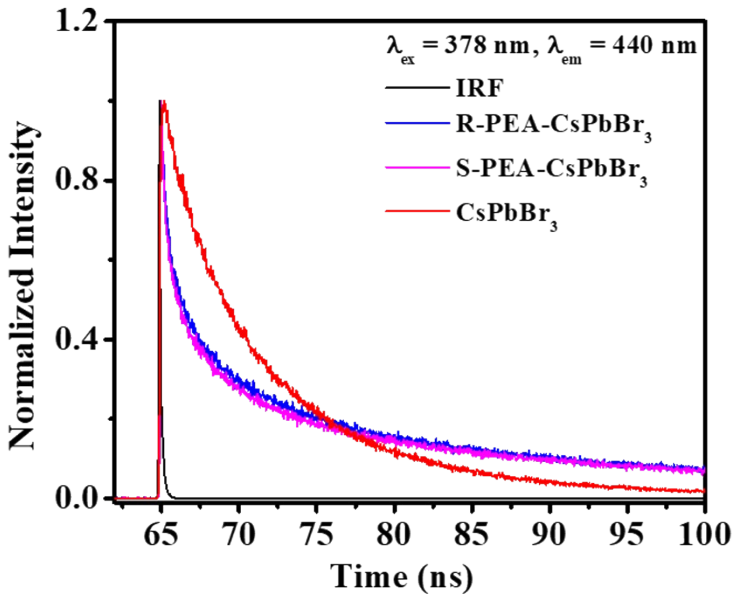

Figure S2. Emission decay profiles (dotted lines) and fits (solid lines) of $CsPbBr_3$ and R- and S-$CsPbBr_3$ NPs in toluene are shown. The PEA concentration was maintained at 10 mM in the NP dispersion.

Table S1. Lifetime Parameters of the Different Nanoparticle (NP) Systems Studied.[1]

System (NP)	a_1	τ_1 (ns)	a_2	τ_2 (ns)	a_3	τ_3 (ns)	$\langle\tau\rangle$ (ns)[2]
$CsPbBr_3$	0.35 ± 0.04	2.20 ± 0.20	0.58 ± 0.03	6.70 ± 0.10	0.07 ± 0.01	17.10 ± 0.20	5.85 ± 0.23
R-/S-PEA-$CsPbBr_3$	0.85 ± 0.08	0.78 ± 0.03	0.10 ± 0.01	5.9 ± 0.07	0.06 ± 0.007	30.0 ± 0.30	3.00 ± 0.30

[1]The decays are fitted to a multiexponential model using the equation $I(t) = \Sigma a_i \exp(-t/\tau)$, where $\Sigma a_i = 1$.

[2]$\langle\tau\rangle = a_1\tau_1 + a_2\tau_2 + a_3\tau_3$ with τ_1, τ_2, and τ_3 being the three lifetime components having relative amplitudes a_1, a_2, and a_3 respectively. $\chi^2 \leq 1.26$.

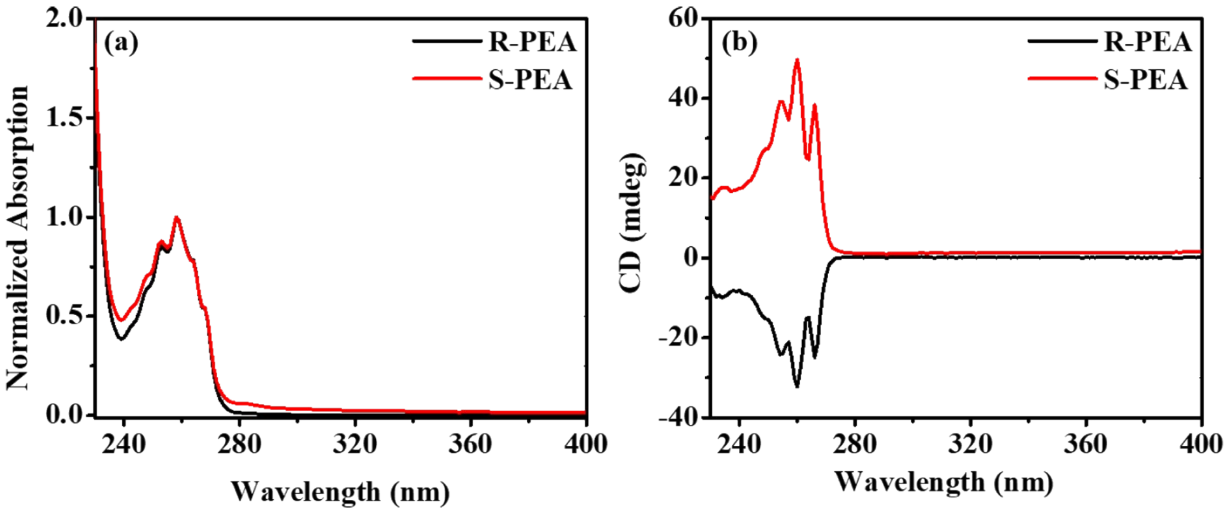

Figure S3. (a) UV-vis absorption and (b) CD spectra of R-(black) and S-PEA (red) in methylcyclohexane.

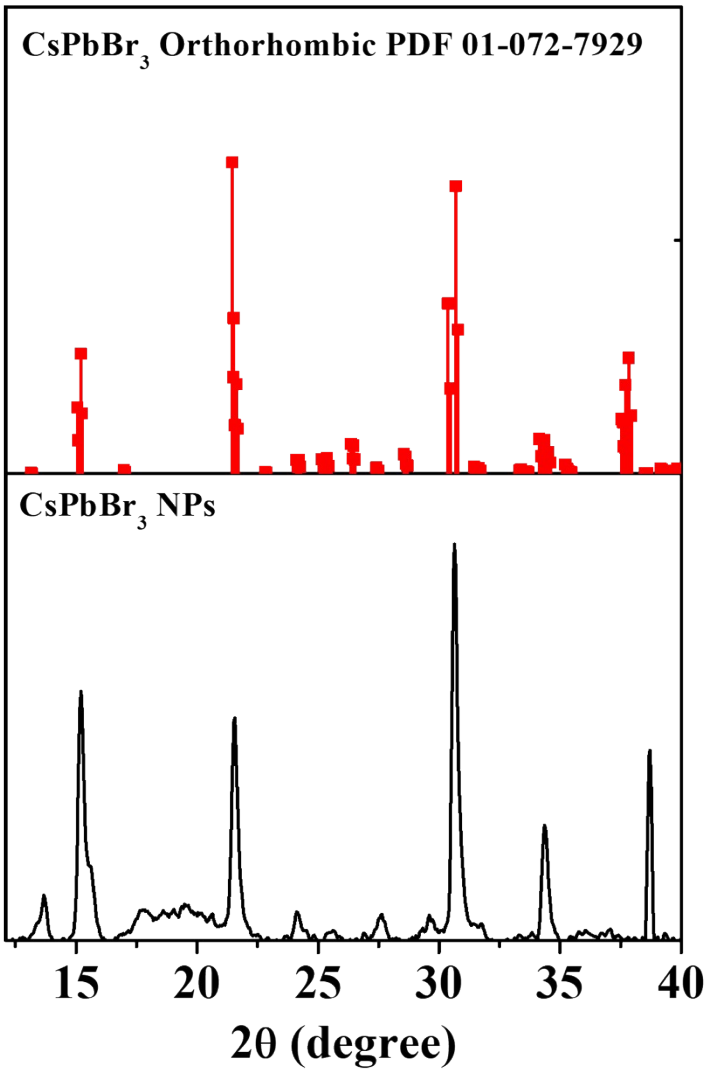

Figure S4. Powder XRD patterns of $CsPbBr_3$ NPs (black) in agreement with an orthorhombic crystal structure (red).

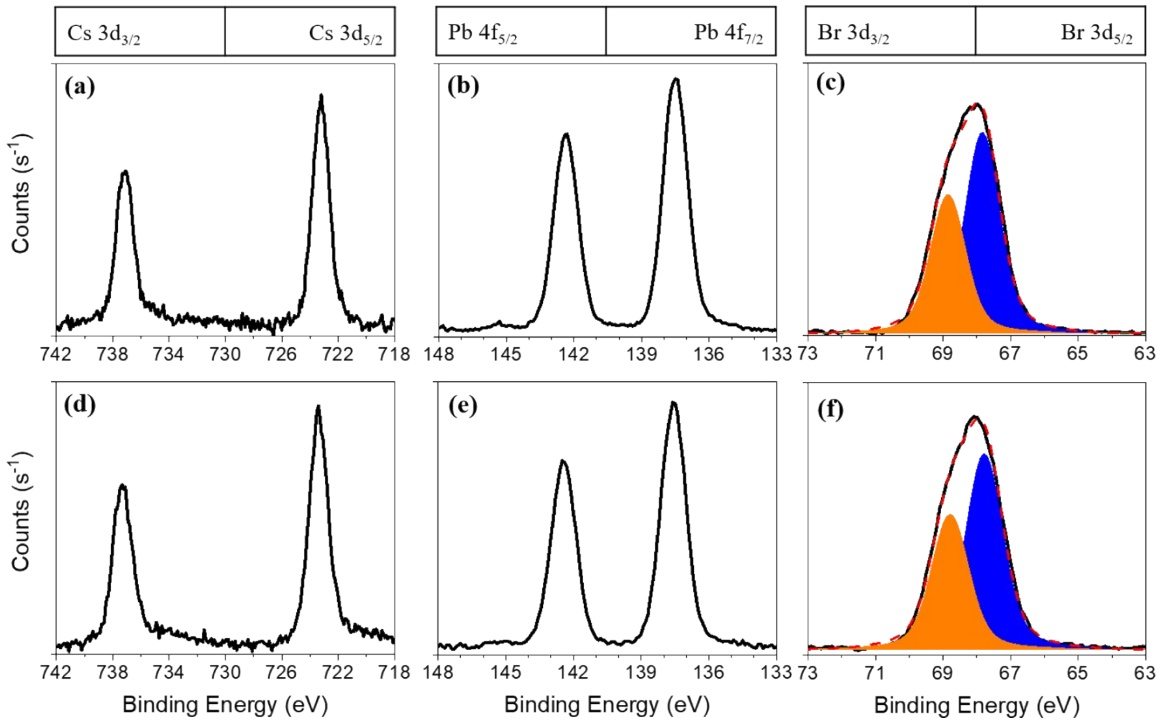

Figure S5. (a) Cs 3d, (b) Pb 4f, (c) Br 3d X-ray photoelectron spectra of the $CsPbBr_3$ NPs along with the corresponding spectra for the R-PEA-$CsPbBr_3$ NPs (d-f) are shown.

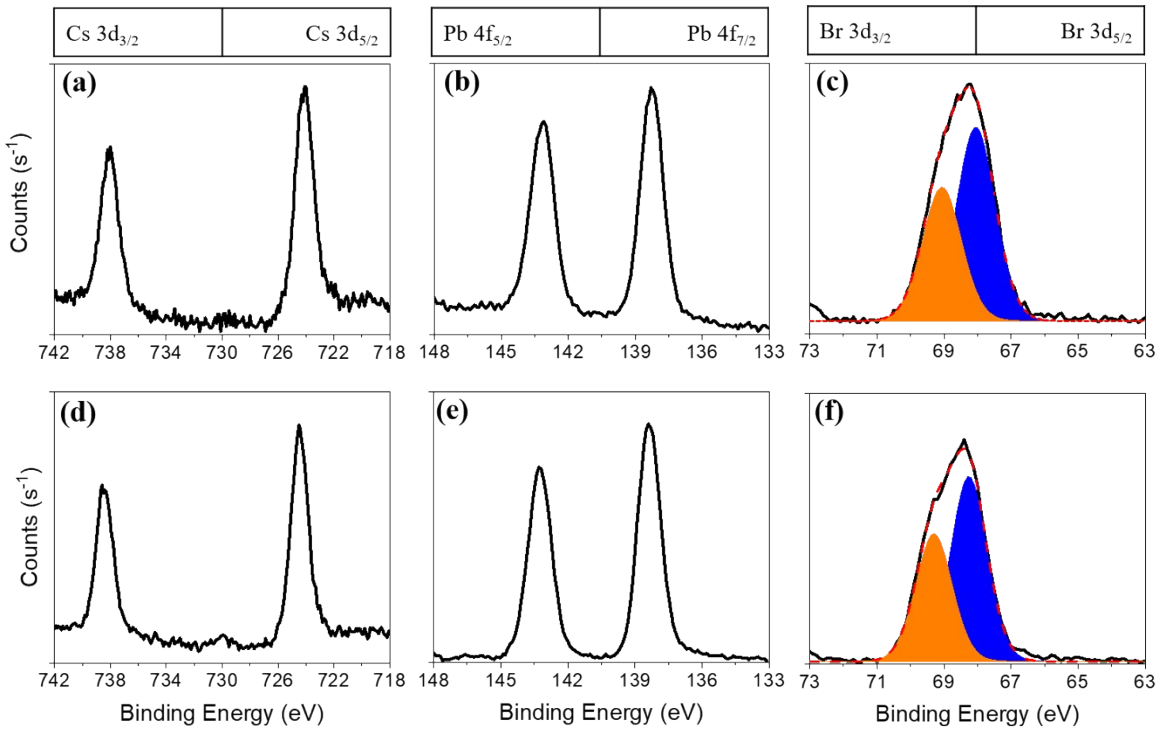

Figure S6. (a) Cs 3d, (b) Pb 4f, (c) Br 3d X-ray photoelectron spectra of R- NEA-$CsPbBr_3$ NPs and (d) Cs 3d, (e) Pb 4f, (f) Br 3d X-ray photoelectron spectra of R-OcAm-$CsPbBr_3$ NPs are shown.

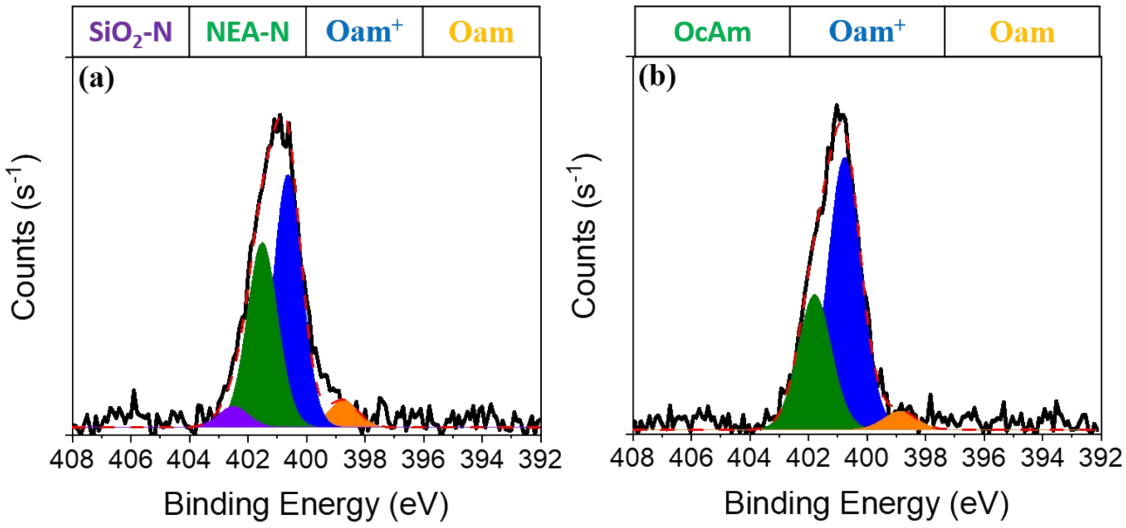

Figure S7. N 1s X-ray photoelectron spectra of (a) R-NEA-$CsPbBr_3$ NPs and (b) R-OcAm-$CsPbBr_3$ NPs are shown. The signal at SiO_2-NEA signal arises from excess ligand interacting with the substrate.

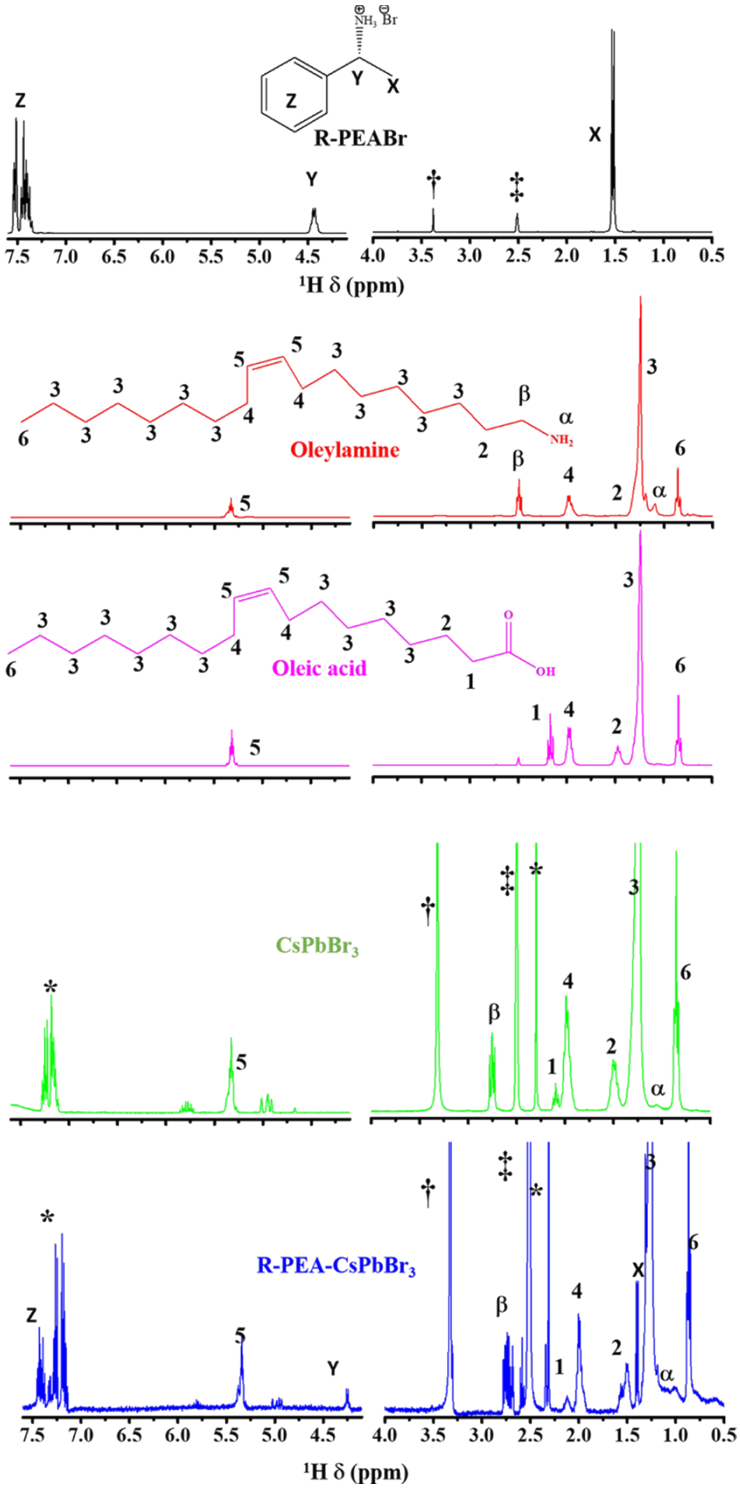

Figure S8. ^{1}H NMR spectra of R-PEABr (black), oleylamine (red), oleic acid (pink), $CsPbBr_3$ (green) and R-PEA-$CsPbBr_3$ (blue) NPs. Residual solvent resonances are marked as *, † and ‡ for toluene, H_2O and DMSO respectively. The inset shows the molecular structure and the corresponding resonance identification of the ligands.

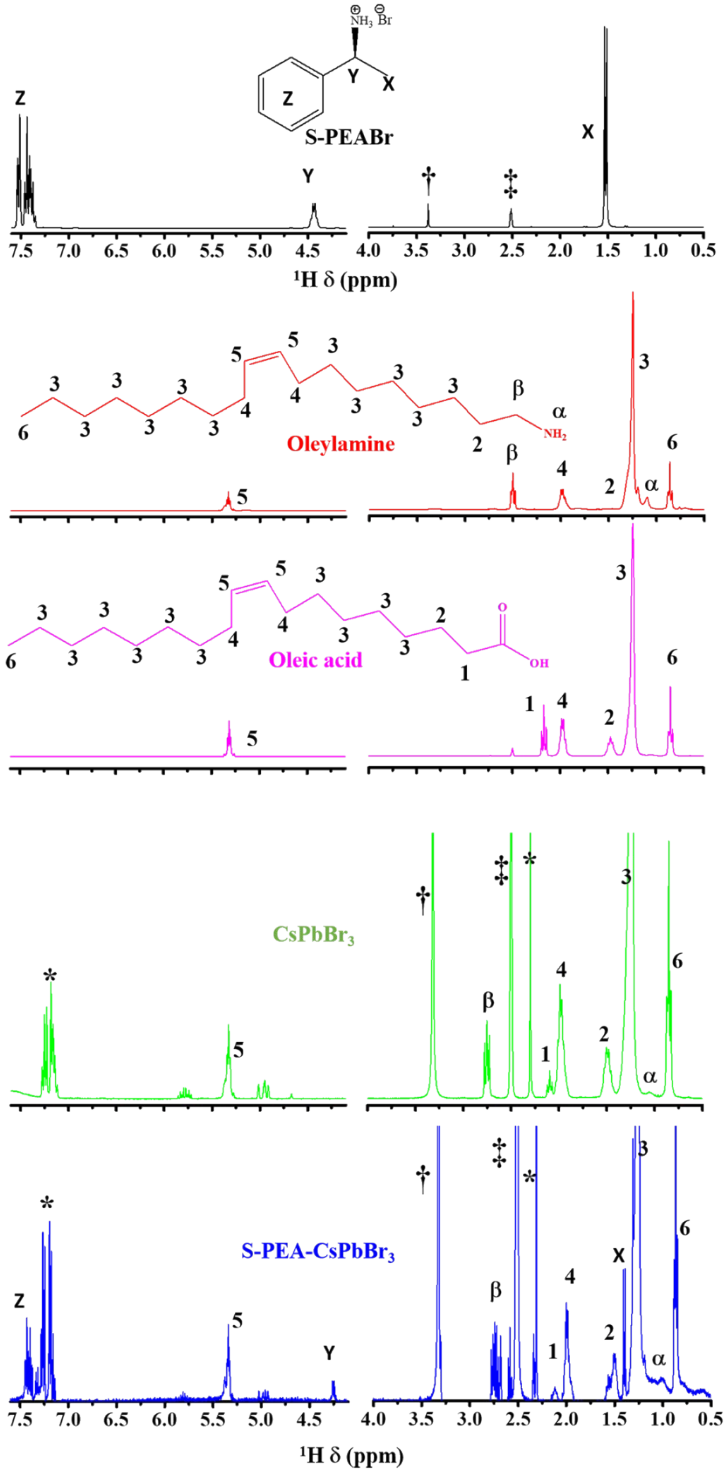

Figure S9. ^{1}H NMR spectra of S-PEABr (black), oleylamine (red), oleic acid (pink), $CsPbBr_3$ (green) and S-PEA-$CsPbBr_3$ (blue) NPs. Residual solvent resonances are marked as *, † and ‡ for toluene, H_2O and DMSO respectively. The inset shows the molecular structure and the corresponding resonance identification of the ligands.

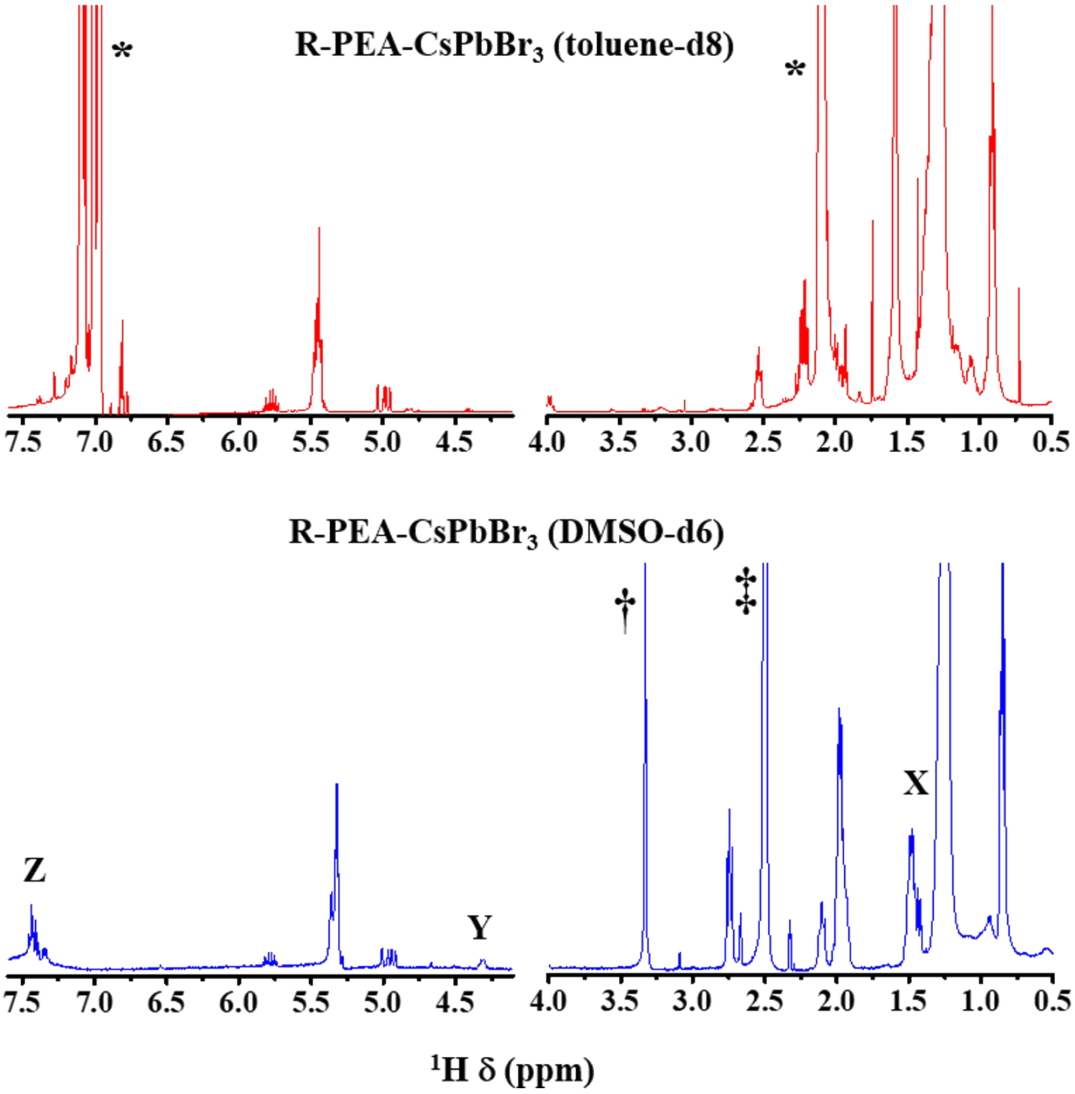

Figure 10. ^{1}H NMR spectra of R-PEA-$CsPbBr_3$ NPs in toluene-d8 (red) and DMSO-d6 (blue) are shown. Residual solvent resonances are marked as *, † and ‡. Contributions from PEA are marked according to the nomenclature in Figure S6.

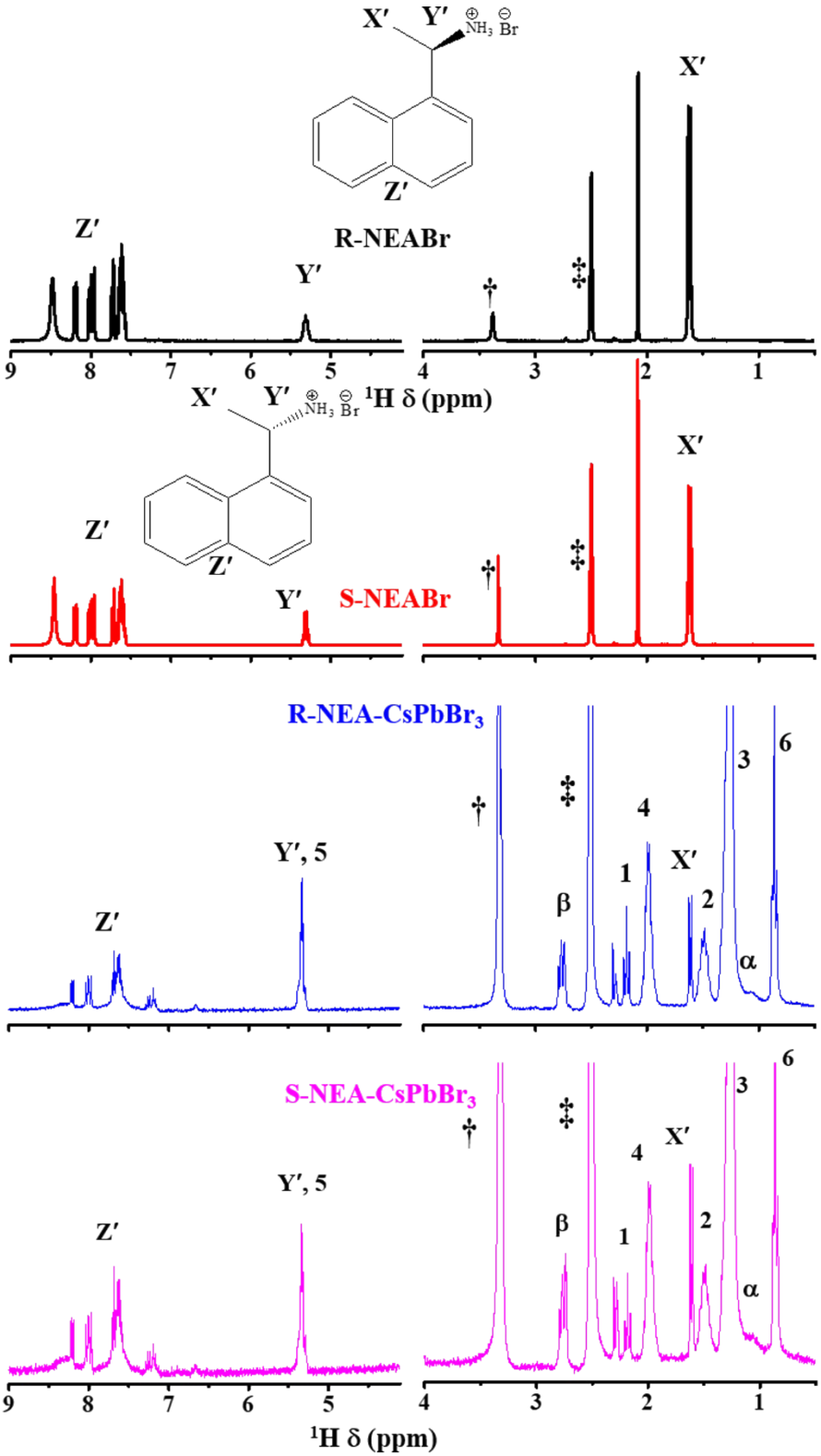

Figure S11. ^{1}H NMR spectra of R- (black) and S-NEABr (red) and R- (blue) and S-NEA-$CsPbBr_3$ (pink) NPs are shown. Contributions from oleic acid and oleylamine are marked according to the nomenclature in Figure S6. Residual solvent resonances are marked as † and ‡.

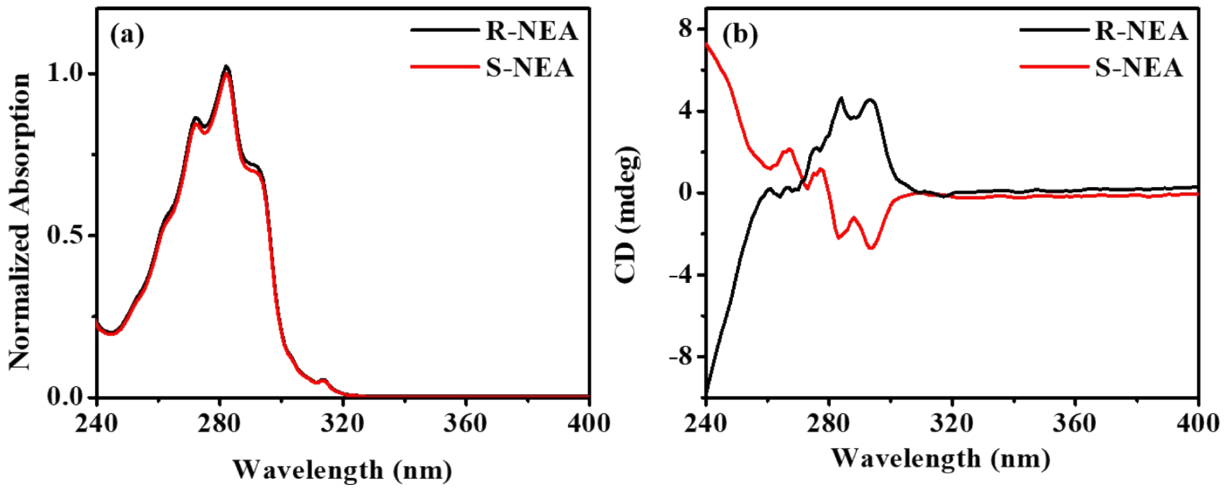

Figure S12. (a) UV-vis absorption and (b) CD spectra of R- (black) and S-NEA (red) in methylcyclohexane.

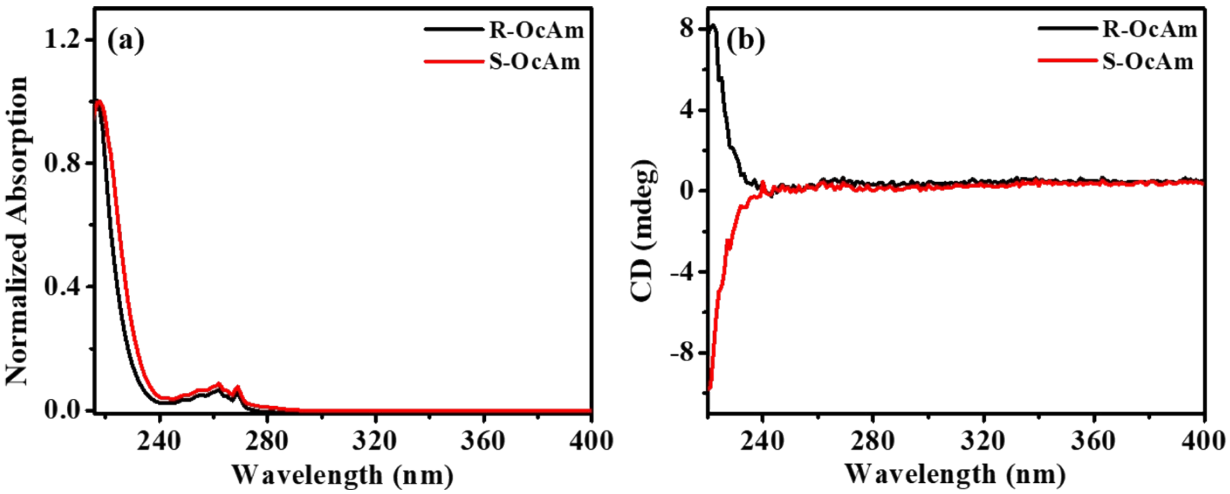

Figure S13. (a) UV-vis absorption and (b) CD spectra of R-(black) and S-OcAm (red) in methylcyclohexane.

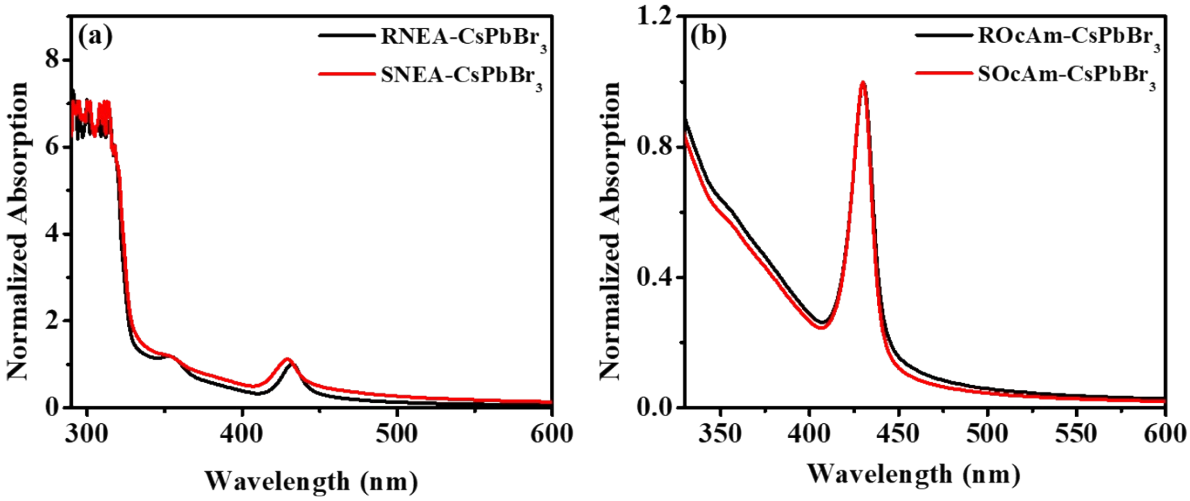

Figure S14. Normalized absorption spectra of (a) R- and S- NEA-$CsPbBr_3$ NPs ([NEA = 30 mM in NP dispersion). The NEA based absorption transition is centered at 300 nm and (b) R- and S-OcAm-$CsPbBr_3$ NPs ([OcAm] = 11 mM in NP dispersion).

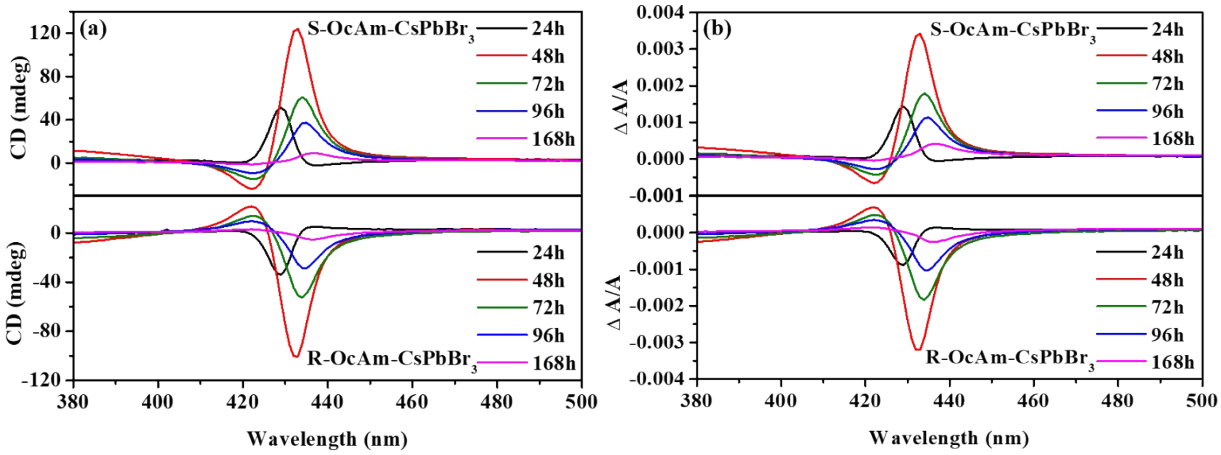

Figure S15. (a) Progression of the CD signals as a function of ligand incubation time and (b) their corresponding representation in terms of ΔA/A are shown for R- and S-OcAm-$CsPbBr_3$ NPs. Note that the R- and S-OcAm have positive and negative CD signals respectively, as shown in Fig. S13 but show a flip in sign for the R- and S-OcAm-$CsPbBr_3$ NPs. This is not unusual and can be explained based on the differences on the coordination geometry of ligands as they interact with the NP surface and has been previously shown to be operative for chiral II-VI semiconductor NPs as well (Nano Lett., 2016, **16**, 4583-4589).

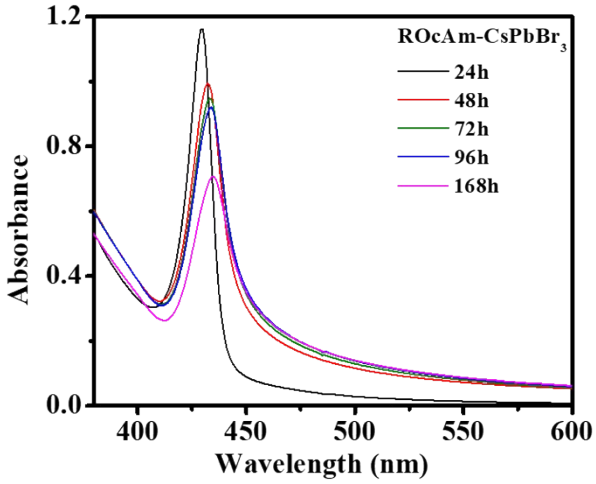

Figure S16. UV-vis absorption spectra of R-OcAm-$CsPbBr_3$ NPs as a function of ligand incubation time.